Ti^{4+}-Immobilized Magnetic Composite Microspheres for Highly Selective Enrichment of Phosphopeptides

Wanfu Ma, Ying Zhang, Lulu Li, Yuting Zhang, Meng Yu, Jia Guo, Haojie Lu, and Changchun Wang**

Architectural design is essential to achieve ideal chemical and biological properties of nanomaterials. In this article, a novel route to fabricate high-quality magnetic composite microspheres composed of a high-magnetic-response magnetic colloid nanocrystal cluster (MCNC) core, a poly(methylacrylic acid) (PMAA) interim layer, and a Ti^{4+}-immobilized poly(ethylene glycol methacrylate phosphate) (PEGMP) shell via two-step distillation–precipitation polymerization is presented. The unique as-synthesized MCNC@PMAA@PEGMP-Ti^{4+} composite microsphere is investigated for its applicability for selective enrichment of phosphopeptides from complex biological samples. The experiment results demonstrate that, by taking advantage of the pure phosphate–Ti^{4+} interface and high Ti^{4+} loading amount, the MCNC@PMAA@PEGMP-Ti^{4+} composite microsphere possesses remarkable selectivity for phosphopeptides even at a very low molar ratio of phosphopeptides/nonphosphopeptides (1:500). The extreme sensitivity, excellent recovery of phosphopeptides, and high magnetic susceptibility are also proven. These outstanding features demonstrate that the MCNC@PMAA@PEGMP-Ti^{4+} composite microspheres have great benefit for the pretreatment before mass spectrometric analysis of phosphopeptides. Furthermore, the performance of the approach in selective enrichment of phosphopeptides from drinking milk and human serum gives powerful evidence for its high selectivity and effectiveness in identifying the low-abundant phosphopeptides from complicated biological samples.

1. Introduction

Multifunctional nanomaterials with designed structures, controlled morphologies, and desirable components have been extensively explored to realize the integration of specific respective functions of the different building blocks or even to achieve cooperatively enhanced performance.[1–12] As an important component type, magnetic composite microspheres have attracted immense interest due to their unique magnetic responsiveness and wide range of current and potential applications in the biomedical field, including uses in bioseparation, medical diagnosis, and magnetically targeted drug delivery.[13–22] They also allow other intricate micromanipulations to be easily performed in complex biological systems simply via the application of an external magnetic field, while particles can also be viewed and followed using MRI tomographic methods.[23–26] Along this line, the application of magnetic composite microspheres to proteomics research has also garnered much attention.[27–32]

Post-translational modifications (PTMs) are chemical modifications of a protein performed in order to broaden its biological functionality. Reversible protein phosphorylation, as one of the most important protein PTMs, plays a vital role in regulating many complex biological processes, such as cellular growth and division, and signaling transduction.[33–35] In order to understand these biological processes, identification of the phosphorylation sites and quantification of their dynamic changes are crucial. Mass spectrometry (MS) has been demonstrated to be the most important and powerful tool for the analysis of protein phosphorylation in view of its ultrahigh sensitivity, wide dynamic range, and superior speed in analyzing mixtures. However, the identification and characterization of phosphoproteins remain challenging due to their low dynamic stoichiometry and the signal suppression of nonphosphorylated peptides. Thus, selective enrichment of phosphoproteins or phosphopeptides from highly complicated mixtures is vital for MS-based phosphoproteome analysis.

Of the various enrichment strategies, immobilized metal affinity chromatography (IMAC), which relies on the affinity of the phosphate groups to metal ions immobilized on a matrix, is the most commonly used technique to fish the phosphorylated peptides out of the pool of predominantly non-phosphorylated peptides. In the early state, iminodiacetic acid (IDA) and

W. F. Ma, Y. T. Zhang, M. Yu, Dr. J. Guo
Prof. C. C. Wang
State Key Laboratory of Molecular Engineering of Polymers and Department of Macromolecular Science, Laboratory of Advanced Materials
Fudan University
Shanghai 200433, China
E-mail: ccwang@fudan.edu.cn
Dr. Y. Zhang, L. L. Li, Prof. H. J. Lu
Department of Chemistry and Institutes of Biomedical Sciences
Fudan University
Shanghai 200032, China
E-mail: luhaojie@fudan.edu.cn

DOI: 10.1002/adfm.201201364

nitrilotriacetic acid (NTA) were selected as the chelating ligands to immobilize Fe^{3+} or Ga^{3+} via the chelation of the metal ions to the carboxylic groups and amino groups on IDA or NTA.[36–38] However, the easy loss of the bound metal ions during sample loading and washing caused by the relatively weaker interaction (each metal ion only coordinates one IDA or NTA ligand) and the serious non-specific adsorption of acidic peptides greatly reduced their specificity for enrichment of phosphopeptides. Recently, metal(IV) phosphate chemistry, using species such as Ti^{4+} and Zr^{4+}, was developed to overcome these obstacles.[39–43] The extremely strong binding (each metal ion coordinates to more than one phosphate molecule) and absolutely pure interface of metal phosphate sites greatly prevent the binding of carboxylic or other peptides and improve the selectivity of phosphopeptides.

Combining magnetic nanomaterials with metal(IV) phosphate chemistry could simultaneously achieve the simple and efficient separation of the phosphopeptides from the peptides mixture by using magnetic separation.[44–46] Unfortunately, these previous reports failed to obtain a pure interface of metal phosphate; impurities such as SiO_2 or C were also present, largely on the surface of the composite microspheres, which definitely influenced the specificity. Therefore, developing new methods to fabricate magnetic composite microspheres with highly pure surfaces of metal phosphate is highly desirable. Herein, for the first time, we rationally design and present a novel synthesis route for preparation of high-quality Ti^{4+}-immobilized MCNC@PMAA@PEGMP composite microspheres involved two-step distillation–precipitation polymerization (DPP).[47] The as-synthesized MCNC@PMAA@PEGMP-Ti^{4+} composite microspheres was proved to have a well-defined core/shell/shell structure, large amount of metal phosphate and high magnetic susceptibility. These composite nanomaterials were investigated in selective enrichment of phosphopeptides, the remarkable selectivity, extreme sensitivity, excellent recovery of phosphopeptides, and high magnetic susceptibility all make the MCNC@PMAA@PEGMP-Ti^{4+} composite microspheres an ideal nanomaterial for mass spectrometric analysis of phosphopeptides. The performance of MCNC@PMAA@PEGMP-Ti^{4+} in selective enrichment of low-abundance phosphopeptides from the tryptic digests of drinking milk and human serum was performed, which clearly demonstrated its great capability in phosphoproteome analysis for real biological samples.

2. Results and Discussion

2.1. Preparation and Characterization of MCNC@PMAA@PEGMP

The protocol for the synthesis of MCNC@PMAA@PEGMP double-shell microspheres with MCNC as core, crosslinked PMAA as interim layer, and crosslinked PEGMP as outer layer is illustrated in **Scheme 1** (Route 1). Briefly, approximately 300 nm sized MCNCs stabilized by citrate were first synthesized by a modified solvothermal reaction. Then the as-prepared MCNCs were modified by MPS to form the available double bonds on the surface of MCNCs for promoting the coating of the robust PMAA layer by distillation–precipitation polymerization (DPP). This interim layer is crucial for the formation of the outer PEGMP shell; it can shield the interaction between the phosphate group of EGMP and Fe_3O_4 of MCNC, which definitely greatly enhanced the stability of the reaction system. Additionally, the strong hydrogen bond between the surface carboxyl group and the phosphate group of EGMP also facilitate the direct coating of PEGMP layer over PMAA layer via the second-step distillation–precipitation polymerization.

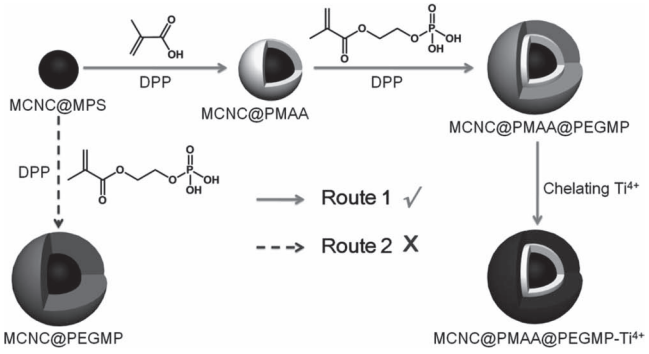

Scheme 1. Schematic illustration of the synthetic procedure for preparation of Ti^{4+}-immobilized MCNC@PMAA@PEGMP core/shell/shell microspheres.

Representative TEM images of MCNCs and MCNC@PMAA core/shell microspheres are shown in **Figure 1**a,b. The MCNCs gave an average diameter of ca. 300 nm, and were

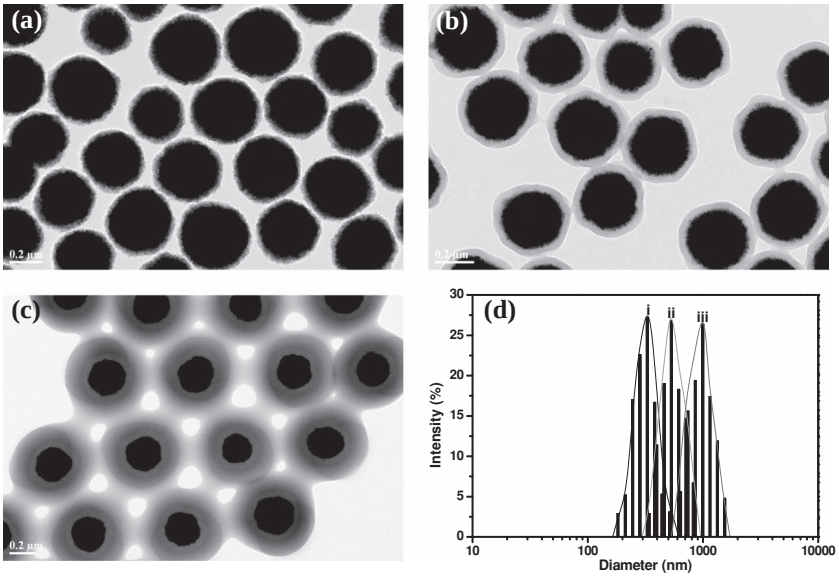

Figure 1. a–c) Representative TEM images of MCNCs, MCNC@PMAA, and MCNC@PMAA@PEGMP, respectively (all scale bars are 200 nm). d) Hydrodynamic diameter distributions of: i) MCNC@MPS, ii) MCNC@PMAA, and iii) MCNC@PMAA@PEGMP.

uniform in both shape and size. After encapsulation with PMAA, the size of the composite microspheres increased to around 390 nm. The obtained MCNC@PMAA micospheres possessed a well-defined core/shell structure and superior dispersibility in many polar solvents, including the reaction solvent of acetonitrile. The hydrodynamic diameters (D_h) and their distribution of MCNCs and MCNC@PMAA microspheres in water compiled in Figure 1d provide additional evidence for the successful coating. The average D_h of MCNCs and MCNC@PMAA are 328 and 566 nm, respectively. In addition, the narrow size distributions (the polydispersity indices for MCNC and MCNC@PMAA were 0.095 and 0.069, respectively) indicate that they all have a good dispersibility in water.

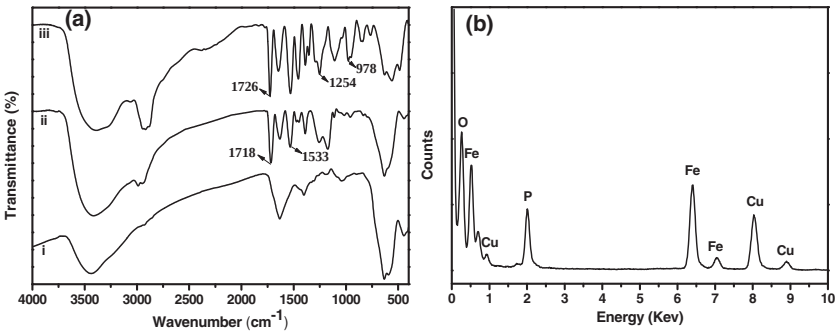

Figure 2. a) FT-IR spectra of i) MCNC@MPS, ii) MCNC@PMAA, iii) MCNC@PMAA@PEGMP. b) EDX spectrum of MCNC@PMAA@PEGMP.

The PMAA layer is essential for the coating of the next PEGMP layer. We tried to directly coat a PEGMP layer onto the MCNC as shown in Scheme 1 (Route 2), but unfortunately it did not work. The main reason is that the phosphate groups of EGMP have strong interactions with the ferrum component of MCNCs, thus a mass of EGMP molecules will adsorb onto the surface of MCNCs when they are mixed together, subsequently seriously influencing the dispersion stability of the MCNCs in the solvent (acetonitrile). Therefore, an appropriate interim layer is required. This interim layer should not only block the contact of MCNCs with the EGMP molecules but also provide certain critical surface properties. On one hand, the surface functional groups should ensure that the seed microspheres have a good dispersibility in the solvent; on the other hand, the matrix ought to give high accessibility to EGMP monomers to achieve a high-quality covering layer of PEGMP. Based on these two considerations, we carefully selected PMAA as the intermediate layer, in which the surface carboxyl groups render the MCNC@PMAA microspheres dispersed very well in acetonitrile, while the easily formed hydrogen bond between the carboxyl group and the phosphate group provides sustainable accessibility of MCNC@PMAA to the EGMP monomer as well as the resulting PEGMP shell.

The superficial functional group density of the magnetic composite microspheres is responsible for the outcome of their biological applications. Typically, in our system, a high surface density of phosphate groups is critical for achieving high performance in selective enrichment of phosphopeptides. In our approach, we realized nearly the highest possible density by copolymerizing EGMP with only a very small quantity of crosslinker of MBA through distillation–precipitation polymerization. Figure 1c shows a typical TEM image of the obtained MCNC@PMAA@PEGMP composite microsphere; the well-defined core/shell/shell structure is distinctly observed (the thin brighter layer is the middle layer of PMAA and the thick dark layer is the PEGMP layer). These composite microspheres can be well-dispersed in water; the discrete and dispersible microspheres are determined by DLS measurements (Figure 1d), which exhibit rather narrow D_h distributions (the PDI was 0.043).

The presence of carboxyl acid groups in the PMAA shell could be proved by FT-IR spectroscopy. As shown in **Figure 2**a, in comparison to the spectrum of MPS-modified MCNCs (MCNC@MPS), new peaks appeared at 1718 and 1533 cm^{-1}, which can be attributed to the stretching vibration of C=O of carboxyl groups and the bending vibration of N–H of MBA. The phosphate groups in the shell could also be demonstrated by the FT-IR spectra (Figure 2a), in which the new peaks appearing at 1726, 1254, and 978 cm^{-1} are ascribed to the stretching vibration of C=O of the ester group of PEGMP, the stretching vibration of P=O of the phosphate group of PEGMP and the asymmetric stretching vibration of P–O–C links of PEGMP, respectively. Energy dispersive X-ray (EDX) spectra were recorded to identify the composition of the core/shell/shell microspheres (Figure 2b). C, P, Fe, and O were the four main elements found, indicating that the obtained microspheres were composed of the target composition.

Thermogravimetric analysis (TGA) (**Figure 3**a) was executed to quantitatively determinate the composition of the composite microspheres. As the organic components decomposed at high temperature while the inorganic components remained, the TGA curves of MCNC@MPS and MCNC@PMAA show the Fe_3O_4 weight percentage of these two microspheres. The 19 wt% loss of MCNC@MPS is attributed to the weight ratio of the citrate stabilizer and a small amount of MPS, indicating the Fe_3O_4 content is 81 wt%. After coating by PMAA layer, the Fe_3O_4 content in composite microspheres

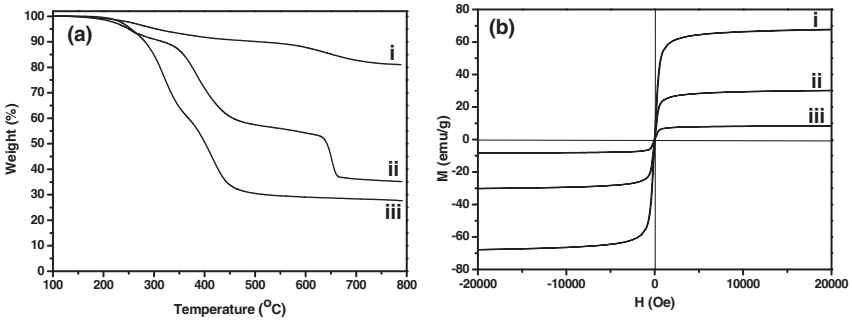

Figure 3. a) TGA curves and b) magnetic hysteresis curves of: i) MCNC@MPS, ii) MCNC@PMAA, and iii) MCNC@PMAA@PEGMP.

dramatically declined to 35.2 wt%. When the outmost PEGMP layer was introduced, the weight loss of the composite microspheres should increase further; the weight loss of MCNC@PMAA@PEGMP was about 72.3 wt%, which is higher than that of MCNC@PMAA (64.8 wt%). However, the weight loss of MCNC@PMAA@PEGMP is not as high as it ought to be, revealing that the PEGMP species decompose incompletely in the N_2 atmosphere, which should be due to the large amount of inorganic element P in the PEGMP species. The MCNC@PMAA@PEGMP composite microspheres decomposed in two main stages (Figure S1 in the Supporting Information). The first stage occurred between 200 and 367 °C, during which the weight loss was about 39.8 wt%. This period involved the disintegration of the organic component of the PEGMP layer. About a 32 wt% loss happened when temperature rose from 367 to 531 °C. During this stage, the PMAA layer and the citrate stabilizer on MCNC were eliminated.

The magnetic properties of the three kinds of microspheres were studied using a vibrating sample magnetometer (VSM; Figure 3b). The magnetic hysteresis curves show that the three kinds of microspheres have no obvious remanence or coercivity at 300 K, indicating that they all possess a superparamagnetic character. The superparamagnetism is coming from the small nanocrystals in the MCNC cores, which behave as superparamagnets. As a control, the saturation magnetization (Ms) value of the MCNCs was measured; it reached 67.5 emu g^{-1}. Upon the coating of the PMAA and PEGMP layer, the Ms values for the MCNC@PMAA and MCNC@PMAA@PEGMP microspheres were reduced to 30.1 and 8.3 emu g^{-1}. Accordingly, the Fe_3O_4 contents of these two composite microspheres were estimated to be 36.1 and 10 wt%, respectively. The accurate content of the PEGMP layer could be estimated to be as high as 72.3 wt%, which gives strong evidence for our hypothesis above, i.e., that the PEGMP species decomposed incompletely in the N_2 atmosphere. In addition, thanks to the high-magnetic-response MCNC core, the final product of MCNC@PMAA@PEGMP microspheres could be separated from the solution in only 30 s when the magnetic field was applied.

2.2. Immobilization of Ti^{4+} onto the Surface of MCNC@PMAA@PEGMP

Immobilization of Ti^{4+} onto the surface of MCNC@PMAA@PEGMP was achieved by the coordination reaction between Ti^{4+} and the phosphate groups of PEGMP via metal(IV) phosphate chemistry. In metal(IV) phosphate chemistry, an α-layered structure of metal(IV) bis(monohydrogen phosphates) is generated by MO_6 octahedra, each one sharing its six oxygen atoms with six different monohydrogen phosphate groups.[48] In turn, each EGMP repeating unit behaves as a bidentate ligand and shares two oxygen atoms with two different metal atoms (**Scheme 2**a). So, each metal ion coordinates to more than one phosphate molecule and each phosphate group also binds to more than one metal ion.

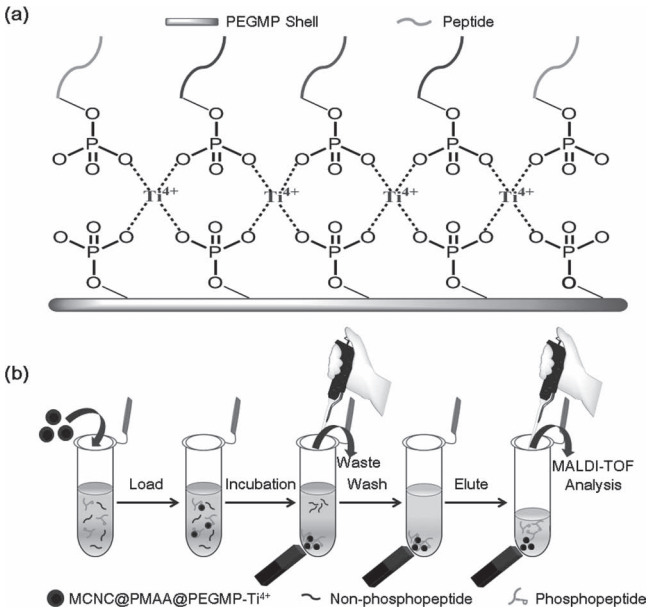

Scheme 2. Scheme illustration of: a) the interaction between Ti^{4+} and the phosphate group of PEGMP or phosphopeptides and b) the typical process for selective enrichment of phosphorylated peptides using MCNC@PMAA@PEGMP-Ti^{4+} microspheres and magnetic separation.

Therefore, the extremely strong binding of the titanium ions provides a very stable, well-defined interface of phosphate–Ti^{4+}, where the located titanium ions are very active and can further react with other exposed phosphate groups,[49] such as the phosphate groups of phosphopeptides.

A representative TEM image of Ti^{4+} immobilized MCNC@PMAA@PEGMP microspheres is shown in **Figure 4**a, in which it can be clearly observed that the core/shell/shell structure was perfect. The scanning TEM (STEM) image (Figure 4b) of a single MCNC@PMAA@PEGMP-Ti^{4+} microsphere, combined with EDX elemental mapping (Figure 4c–e), clearly reveals the core/shell/shell structure with a magnetite core, an interim layer and an outer shell, wherein Fe is distributed in the core while Ti and P are spread in the whole outer shell. This result verifies the interaction of Ti^{4+} and the phosphate group of PEGMP, which also suggests that the MCNC@PMAA@PEGMP-Ti^{4+} microspheres may have a high loading amount of

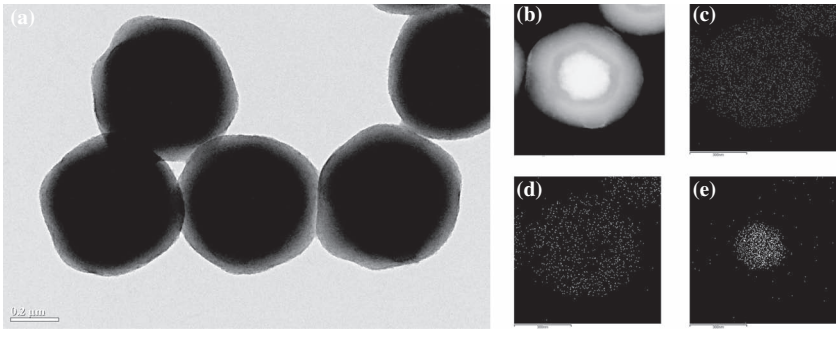

Figure 4. a) Representative TEM image and b) STEM image of MCNC@PMAA@PEGMP-Ti^{4+}. c–e) EDX elemental maps of Ti, P, and Fe, respectively.

Ti^{4+}. The amount of Ti^{4+} was further quantified to be as high as 4.1 wt% by atomic absorption spectrum (AAS).

2.3. Evaluation of Phosphopeptides Enrichment Ability Using Tryptic Digests from Standard Proteins

Based on the metal(IV) phosphate chemistry, immobilized metal affinity chromatography adsorbents, i.e., immobilized Ti^{4+} or Zr^{4+} affinity chromatography adsorbent, have been reported to selective enrich phosphopeptides from complex mixtures.[40–46] Therefore, in light of the unique characters of the synthesized MCNC@PMAA@PEGMP-Ti^{4+} microspheres, we investigated their applicability in selective enrichment of phosphopeptides using the tryptic digests of a standard phosphoprotein β-casein. In a typical enrichment procedure (Scheme 2b), the β-casein digests was incubated with MCNC@PMAA@PEGMP-Ti^{4+} microspheres in a 100 μL loading buffer consisting of 50% acetonitrile containing 1% trifluoroacetic acid. After separation of the microspheres using an external magnetic field and thorough washing with the loading buffer, the trapped phosphopeptides were eluted with 10 μL 5% $NH_3 \cdot H_2O$, and 1 μL of this solution was used for MALDI-TOF MS analysis. For comparison, direct analysis of the β-casein digests was also performed by MS analysis, with the result presented in **Figure 5**a. Without the pretreatment procedure, the obtained spectrum was dominated by non-phosphopeptides, and their presence led to a low signal-to-noise ratio for the phosphopeptides. However, after selective enrichment with MCNC@PMAA@PEGMP-Ti^{4+} microspheres (Figure 5b), signals could be clearly observed for the β-casein phosphopeptides (β1, β2, β3), along with their doubly charged phosphorylated peptides and dephosphorylated counterparts, which were likely formed during the MALDI ionization process. The detailed information of the detected phosphopeptides from tryptic digests of β-casein by MALDI-TOF mass analysis is listed in Table S1 (see Supporting Information). This result demonstrated the selectivity of MCNC@PMAA@PEGMP-Ti^{4+} microspheres toward phosphopeptides.

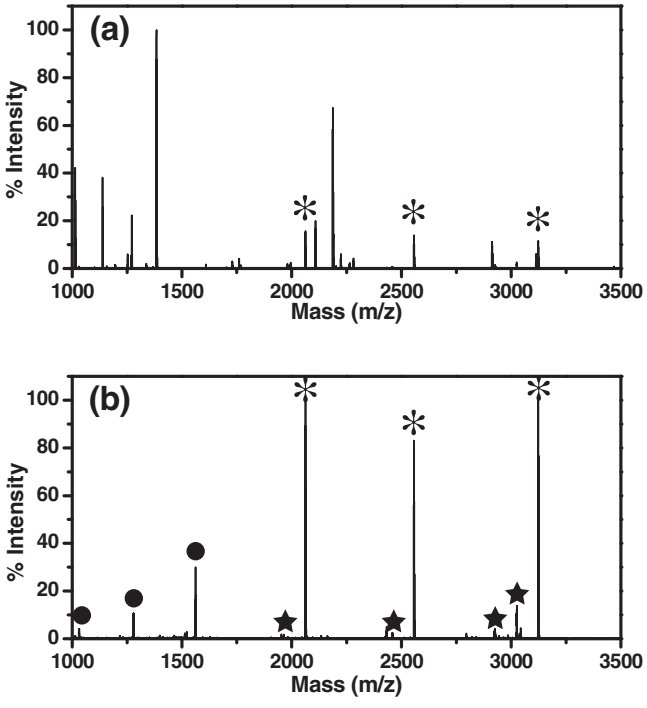

Figure 5. MALDI mass spectra of the tryptic digests of β-casein: a) direct analysis and b) analysis after enrichment using MCNC@PMAA@PEGMP-Ti^{4+}. * indicates phosphorylated peptides, ★ indicates their dephosphorylated counterparts, and ● indicates their doubly charged phosphorylated peptides.

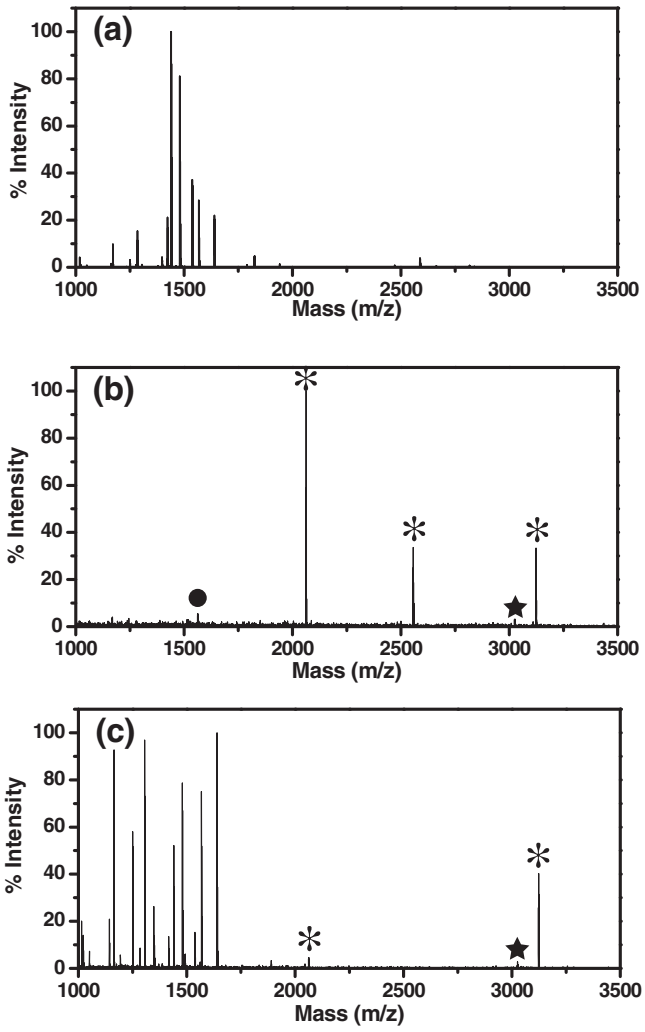

Figure 6. MALDI mass spectra of the tryptic digests mixture of β-casein and BSA (with a molar ratio of β-casein to BSA of 1:500): a) direct analysis, b) analysis after enrichment using MCNC@PMAA@PEGMP-Ti^{4+}, and c) analysis after enrichment using commercial IMAC product. * and ★ indicate phosphorylated peptides and their dephosphorylated counterparts, respectively.

To further evaluate their ability to capture phosphopeptides in complex samples, large amounts of tryptic digests of BSA were added to the tryptic digests of β-casein (the molar ratio of BSA to β-casein is as high as 500:1) to construct a mimic biological sample. As shown in **Figure 6**a, due to the presence of high-abundance non-phosphopeptides (from the BSA), no phosphopeptides were detected before enrichment. However,

after incubation with MCNC@PMAA@PEGMP-Ti^{4+}, all the three phosphopeptides could be easily detected, with a very clean background in the mass spectrum (Figure 6b). As a comparison, when the commercial IMAC product was used, the efficacy of the enrichment was inferior (Figure 6c), with lower phosphopeptide intensities, and non-phosphopeptide peaks dominating the spectrum. To the best of our knowledge, this is the highest enrichment selectivity of magnetic IMAC hitherto reported, which is much better than the previously reported metal(IV) phosphate-functionalized magnetic microspheres[44–46] (Wei,[44] Qi,[45] and Lu et al.[46] demonstrated their materials could achieve good selectivity from a mixture of phosphopeptides and non-phosphopeptides with their molar ratios of 1:20, 1:25, and 1:50, respectively) and the commercial IMAC products. We attribute this unprecedented selectivity to the high purity of the phosphate–Ti^{4+} surface and high density of metal ions.

The capacity, sensitivity and post-enrichment recovery of MCNC@PMAA@PEGMP-Ti^{4+} microspheres toward phosphopeptides were also investigated. To estimate the capacity for phosphopeptide, tryptic β-casein digests at different concentrations with a fixed volume (100 μL) were enriched using the same amount of MCNC@PMAA@PEGMP-Ti^{4+} and then the flow-through fractions were analyzed using matrix-assisted laser desorption/ionization time-of-flight (MALDI-TOF) MS. When the total amount of phosphopeptides was higher than the capacity of the materials, the phosphopeptide signal could be detected. According to this method, the enrichment capacity of MCNC@PMAA@PEGMP-Ti^{4+} was calculated to be about 75 mg g^{-1}. The high detection sensitivity of this approach was demonstrated by the MALDI mass spectrum, shown in **Figure 7**a. The targeted phosphopeptide could be detected at signal-to-noise ratios of 14, 10, and 5 for phosphpeptide with m/z of 2061.83, 2556.09, and 3122.27, respectively, even when the total amount of β-casein was decreased to only 50 fmol. This indicated that the detection limit of this method was at the fmol level. The post-enrichment recovery was investigated by using the ^{18}O labeling method. A certain amount of standard phosphopeptide (pSADGQHAGGLVK) was divided equally into two parts. The first part was treated with immobilized trypsin (homemade) in $H_2{}^{18}O$, which produced a 4 Da mass increase by introducing two ^{18}O atoms at the C-termini of the peptides. The second part was applied in our trap-and-release strategy. By mixing the two parts, we could profile the product with MS to make a comparative study of the abundances of the phosphopeptides from different oxygen isotopes, according to the peak relative intensities.[50] As the MALDI mass spectrum in Figure 7b reveals, the recovery of phosphopeptides from the MCNC@PMAA@PEGMP-Ti^{4+} microspheres was as high as 87%. These tests lead us to believe that the MCNC@PMAA@PEGMP-Ti^{4+} microspheres act as an ideal magnetic IMAC adsorbent for phosphopeptides with remarkable selectivity, extreme sensitivity, and high enrichment recovery.

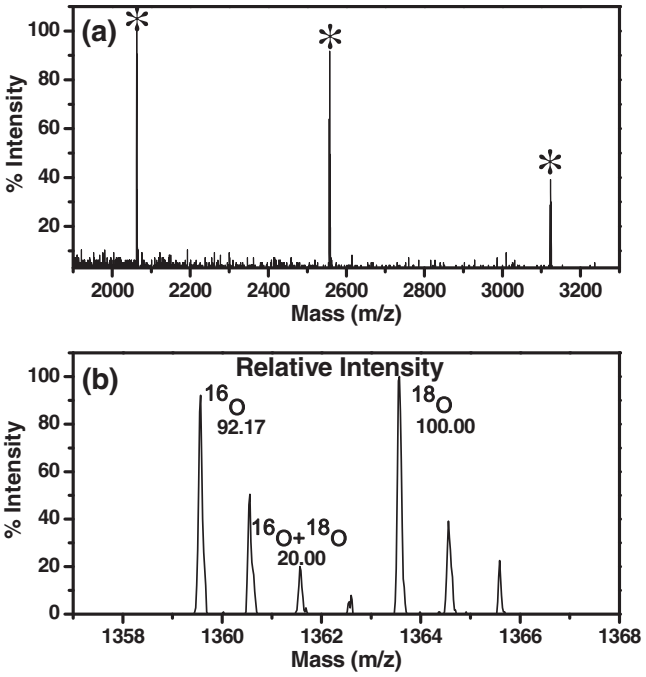

Figure 7. a) MALDI mass spectrum of a tryptic digests of β-casein (0.5 nM, 100 μL), after enrichment. b) MALDI mass spectrum of phosphopeptide pSADGQHAGGLVK (a mixture of unlabeled enriched and an equal amount of ^{18}O-labeled unenriched, used as a control). * indicates phosphorylated peptides.

2.4 Highly Specific Enrichment of Phosphopeptides from Milk and Human Serum

Encouraged by its unique properties, we used drinking milk and human serum to further examine the selectivity and effectiveness of MCNC@PMAA@PEGMP-Ti^{4+} microspheres in the enrichment of low-abundant phosphopeptides from real complex samples. **Figure 8**a display the direct analysis of the tryptic digests of milk with a fat content of about 3%, in which non-phosphopeptides dominated the spectrum and only two weak peaks were generated from phosphopeptides. After treating with MCNC@PMAA@PEGMP-Ti^{4+} (Figure 8b), 10 phosphopeptides with considerable intensities were confidently identified with a clear background. The human serum sample was also used for testing the specificity in enrichment of endogenous low-abundant phosphopeptides. The direct analysis of the human serum is not shown here because of the significant suppression of ionization in MALDI due to the presence of extremely high concentrations of salts. After simultaneously desalting and selective enrichment by MCNC@PMAA@PEGMP-Ti^{4+} microspheres, four peaks of phosphopeptides could be distinctly isolated from the extremely complicated biological system (Figure 8c). For clarity, detected phosphopeptides from the tryptic digests of milk and from human serum are listed in Table S2 and S3 (see Supporting Information). These results clearly indicate the high selectivity and effectiveness of our approach in enrichment of phosphopeptides from real biological samples. Moreover, the inherent capability of convenient enrichment by magnetic separation is the great additional advantage, because otherwise it will need high-speed centrifugation (up to 16 000 rpm) and high-molecular-weight non-phosphopeptides or other impurities may be sedimented during this process.

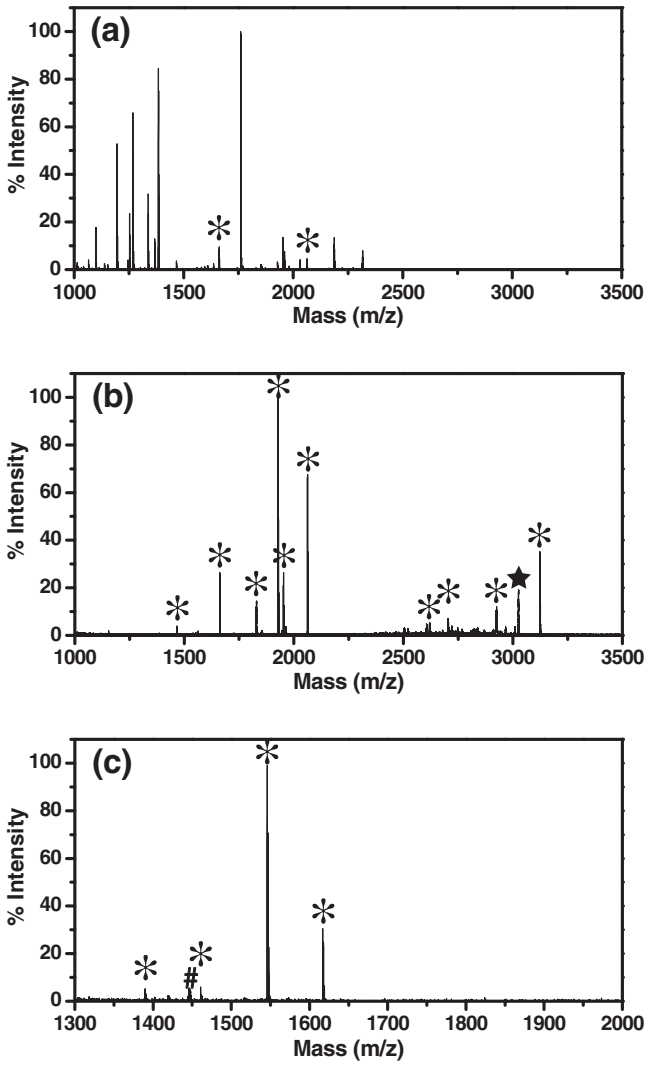

Figure 8. a,b) MALDI mass spectra of the tryptic digests of the milk before and after enrichment by MCNC@PMAA@PEGMP-Ti^{4+}, respectively. c) MALDI-TOF spectrum of human serum after enrichment by MCNC@PMAA@PEGMP-Ti^{4+}. * indicates phosphorylated peptides, ★ and # indicates their dephosphorylated and dehydration counterparts.

3. Conclusions

In summary, we have presented a new facile, repeatable, and mass spectrometry-friendly synthetic route for preparation of magnetic MCNC@PMAA@PEGMP-Ti^{4+} composite microspheres with well-defined core/shell/shell structure, highly pure phophonate–Ti^{4+} interfaces, and high Ti^{4+} content. The PMAA interim layer plays an important role in the successful preparation of the target nanomaterial. The experiments enriching phosphopeptides from mimic biological samples indicated that the MCNC@PMAA@PEGMP-Ti^{4+} microspheres had excellent performance for selective enrichment of phosphopeptides. What's more, the effect of selective enrichment of phosphopepetides from drinking milk and human serum further demonstrated its capability in identifying low-abundance phosphopeptides from real complex samples. We also believe that the MCNC@PMAA@PEGMP microspheres have great potential for removing heavy metals from aqueous solution and also some other biomedical applications.

4. Experimental Section

Materials: Iron(III) chloride hexahydrate ($FeCl_3{\cdot}6H_2O$), ammonium acetate (NH_4Ac), ethylene glycol (EG), anhydrous ethanol, trisodium citrate dihydrate, aqueous ammonia solution (25%), and methylacrylic acid (MAA) were purchased from Shanghai Chemical Reagents Company and used as received. *N,N′*-methylenebisacrylamide (MBA) was bought from Fluka and recrystallized from acetone. 2,2-azobisisobutyronitrile (AIBN), and $Ti(SO_4)_2$ were supplied by Sinopharm Chemical Reagents Company. γ-Methacryloxypropyltrimethoxysilane (MPS) was obtained from Jiangsu Chen Guang Silane Coupling Reagent Co., Ltd. Ethylene glycol methacrylate phosphate (EGMP), β-casein, bovine serum albumin (BSA, 95%), 2,5-dihydroxybenzoic acid (2,5-DHB, 98%), ammonium bicarbonate (ABC, 99.5%), and 1-1-(tosylamido)-2-phenylethyl chloromethyl ketone (TPCK)-treated trypsin (E.G 2.4.21.4) were purchased from Sigma (St. Louis, MO). Acetonitrile (ACN, 99.9%) and trifluoroacetic acid (TFA, 99.8%) were purchased from Merck (Darmstadt, Germany). Phosphoric acid (85%) was purchased from Shanghai Feida Chemical Reagents Ltd. (Shanghai, China). Matrix DHB was dissolved in acetonitrile/water/H_3PO_4 (50:49:1, v/v/v) solution by keeping DHB at 10 mg mL^{-1}. Commercial IMAC product was prepared by immersion POROS MC 20 μm Self Pack Media (from Applied Biosystems, USA) in $FeCl_3$ (100 mM) for 30 min. Milk was purchased from a local market. Deionized water (18.4 MΩ cm) used for all experiments was obtained from a Milli-Q system (Millipore, Bedford, MA).

Synthesis of MCNC@PMAA Core/Shell Microspheres: The magnetic MCNC@PMAA core/shell microspheres were prepared according to our prior work.[51] The magnetite colloidal nanocrystal clusters (MCNCs) were prepared through a modified solvothermal reaction. Typically, $FeCl_3{\cdot}6H_2O$ (1.350 g), NH_4Ac (3.854 g) and sodium citrate (0.4 g) were dissolved in ethylene glycol (70 mL). The mixture was stirred vigorously for 1 h at 170 °C to form a homogeneous black solution, and then transferred into a Teflon-lined stainless-steel autoclave (100 mL capacity). The autoclave was heated at 200 °C and maintained for 16 h, and then it was cooled to room temperature. The black product was washed with ethanol and collected with the help of a magnet. The cycle of washing and magnetic separation was repeated for several times. The final product was dispersed in ethanol for further use.

Modification of MCNCs with MPS was achieved by adding ethanol (40 mL), deionized water (10 mL), $NH_3{\cdot}H_2O$ (1.5 mL), and MPS (0.3 g) into the MCNCs ethanol suspension and vigorously stirring the mixture for 24 h at 60 °C. The obtained product was separated by using a magnet and washed with ethanol to remove excess MPS. The resultant MCNC@MPS nanoparticles were dried in a vacuum oven at 40 °C till constant weight.

Coating the PMAA layer onto MCNC@MPS nanoparticles was executed by distillation-precipitation polymerization of MAA, with MBA as the cross-linker and AIBN as the initiator, in acetonitrile. Typically, MCNC@MPS seed nanoparticles (200 mg) were dispersed in acetonitrile (160 mL) in a dried single-necked flask (250 mL capacity) with the aid of an ultrasonicator. Then a mixture of MAA (1.2 mL), MBA (300 mg), and AIBN (30 mg) were added to the flask to initiate the polymerization. The flask, submerged in a heating oil bath, was attached to a fractionating column, Liebig condenser, and a receiver. The reaction mixture was heated from ambient temperature to the boiling state within 30 min and the reaction was ended after about one half of the solvent was distilled from the reaction mixture within 1 h. The obtained MCNC@PMAA microspheres were collected by magnetic separation and washed with ethanol in order to eliminate excess reactants and few generated polymer microspheres.

Synthesis of MCNC@PMAA@PEGMP Core/Shell/Shell Microspheres: MCNC@PMAA@ PEGMP core/shell/shell microspheres were

synthesized with the aid of a hydrogen-bonding interaction between the carboxyl group of PMAA and the phosphate group of EGMP via distillation–precipitation polymerization, in which MCNC@PMAA microspheres were used as seed microspheres. Typically, MCNC@PMAA seed microspheres (100 mg) were dispersed in acetonitrile (100 mL) in a dried single-necked flask (150 mL capacity) with the aid of an ultrasonicator. Then a mixture of EGMP (0.6 mL), MBA (150 mg), and AIBN (15 mg) were added to the flask to initiate the polymerization. The procedure for the polymerization and post-treatment of the resultant MCNC@PMAA@PEGMP microspheres were similar to that of MCNC@PMAA microspheres.

Synthesis of MCNC@PMAA@PEGMP-Ti^{4+}: The Ti^{4+}-immobilized MCNC@PMAA@PEGMP microspheres were obtained by incubation of MCNC@PMAA@PEGMP microspheres (20 mg) in $Ti(SO_4)_2$ solution (100 mM) at room temperature overnight under gentle stirring. The obtained MCNC@PMAA@PEGMP-Ti^{4+} microspheres was collected by magnetic separation and washed with distilled water several times to remove residual titanium ions. The obtained MCNC@PMAA@PEGMP-Ti^{4+} microspheres were dispersed in distilled water before use.

Preparation of Tryptic Digests of Standard Proteins: β-casein and BSA were each dissolved in ABC (25 mM) at pH 8.0 (1 mg mL^{-1} for each protein) and denatured by boiling for 10 min. Protein solutions were then incubated with trypsin at an enzyme/substrate ratio of 1:40 (w/w) for 12 h at 37 °C to produce proteolytic digests, respectively. The tryptic peptide mixtures were stored at –20 °C until further use.

Preparation of Tryptic Digests of Proteins Extracted from Drinking Milk: Drinking milk (30 µL) was diluted in ABC (25 mM, 900 µL). This solution was then centrifugated at 16 000 rpm for 15 min, and the supernatant was saved for tryptic digestion. After denaturation at 100 °C for 10 min, the supernatant was incubated for 8 h at 37 °C with trypsin (30 µg) for proteolysis. This tryptic digests of milk was diluted by ACN/H_2O/TFA (50:49:1, v/v/v) for further use.

Sample Preparation of Human Serum: Serum for the experiments was collected from patient with colorectal cancer with IRB approved protocol from Fudan University Shanghai Cancer Center. Loading buffer (50% ACN containing 1% TFA, 22.5 µL) were added to serum (2.5 µL), followed by gentle mixing for 30 min at room temperature. The sample was votexed for 15 min at 1000 rpm, and then the supernatant was collected for further phosphopeptides enrichment.

Selective Enrichment of Phosphopeptides with MCNC@PMAA@PEGMP-Ti^{4+} Microspheres: The obtained MCNC@PMAA@PEGMP-Ti^{4+} microspheres was first washed with ethanol for three times and then suspended in deionized water (10 mg mL^{-1}). Tryptic digests of β-casein and BSA or proteins extracted from drinking milk were dissolved in loading buffer (50% ACN containing 1% TFA, 100 µL), then MCNC@PMAA@PEGMP-Ti^{4+} microspheres (2 µL) was added and incubated at room temperature for 60 min, respectively. After that, MCNC@PMAA@PEGMP-Ti^{4+} microspheres with captured phosphopeptides was separated from the mixed solutions by applying an external magnet. After washing with loading buffer (200 µL) to remove the non-specifically adsorbed peptides, the trapped phosphopeptides were eluted with $NH_3 \cdot H_2O$ (5%, 10 µL) for further MS analysis.

MALDI Mass Spectrometry: The eluate (1 µL) was deposited on the MALDI probe, and then DHB matrix solution (1 µL) was deposited for MS analysis. MALDI-TOF mass spectrometry analysis was performed in positive reflection mode on a 5800 Proteomic Analyzer (Applied Biosystems, Framingham, MA, USA) with a Nd: YAG laser at 355 nm, a repetition rate of 200 Hz and an acceleration voltage of 20 kV. The range of laser energy was optimized to obtain good resolution and signal-to-noise ratio (S/N) and kept constant for further analysis. External mass calibration was performed by using standard peptides from myoglobin digests.

Characterization: Field-emission transmission electron microscopy (FE-TEM) images were taken on a JEM-2100F transmission electron microscope at an accelerating voltage of 200 kV. Fourier transform infrared (FT-IR) spectra were determined on a NEXUS-470 FT-IR spectrometer over potassium bromide pellet and the diffuse reflectance spectra were scanned over the range of 400–4000 cm^{-1}. Thermogravimetric analysis (TGA) measurements were performed on a Pyris 1 TGA instrument. All measurements were taken under a constant flow of nitrogen of 40 mL min^{-1}. The temperature was first increased from room temperature to 100 °C and held until constant weight, and then increased from 100 to 800 °C at a rate of 20 °C min^{-1}. Magnetic characterization was carried out with a vibrating sample magnetometer (VSM) on a Model 6000 physical property measurement system (Quantum, USA) at 300K. Hydrodynamic diameter (D_h) measurements were conducted by dynamic light scattering (DLS) with a ZEN3600 (Malvern, UK) Nano ZS instrument using He-Ne laser at a wavelength of 632.8 nm.

Supporting Information

Supporting Information is available from the Wiley Online Library or from the author.

Acknowledgements

W.M. and Y.Z. contributed equally to this work. This work was supported by the National Science and Technology Key Project of China (2012CB910602 and 2012AA020204), the National Science Foundation of China (Grant No. 20974023, 21025519, 21128001 and 51073040), Shanghai Projects (10XD1400500, 11XD1400800, Eastern Scholar, and B109), and the Innovation Foundation for Distinguished Students of Fudan University (11-25-15).

Received: May 20, 2012
Revised: July 3, 2012
Published online: August 10, 2012

[1] T. Pellegrino, S. Kudera, T. Liedl, A. M. Javier, L. Manna, W. J. Parak, *Small* **2005**, *1*, 48.
[2] J. Kim, Y. Piao, T. Hyeon, *Chem. Soc. Rev.* **2009**, *38*, 372.
[3] J. H. Gao, H. W. Gu, B. Xu, *Acc. Chem. Res.* **2009**, *42*, 1097.
[4] S. Mann, *Nat. Mater.* **2009**, *8*, 781.
[5] T. J. Yoon, J. S. Kim, B. G. Kim, K. N. Yu, M.-H. Cho, J. K. Lee, *Angew. Chem.* **2005**, *117*, 1092; *Angew. Chem. Int. Ed.* **2005**, *44*, 1068.
[6] J. H. Gao, G. L. Liang, J. S. Cheung, Y. Pan, Y. Kuang, F. Zhao, B. Zhang, X. X. Zhang, E. X. Wu, B. Xu, *J. Am. Chem. Soc.* **2008**, *130*, 11828.
[7] M. Liong, J. Lu, M. Kovochich, T. Xia, S. G. Ruehm, A. E. Nel, F. Tamanoi, J. I. Zink, *ACS Nano* **2008**, *2*, 889.
[8] S. L. Gai, P. P. Yang, C. X. Li, W. X. Wang, Y. L. Dai, N. Niu, J. Lin, *Adv. Funct. Mater.* **2010**, *20*, 1166.
[9] C. G. Wang, J. Irudayaraj, *Small* **2010**, *6*, 283.
[10] S. M. Lee, H. Park, K. H. Yoo, *Adv. Mater.* **2010**, *22*, 4049.
[11] S. P. Sherlock, S. M. Tabakman, L. M. Xie, H. J. Dai, *ACS Nano* **2011**, *5*, 1505.
[12] W. T. Wu, J. Shen, P. Banerjee, S. Q. Zhou, *Adv. Funct. Mater.* **2011**, *21*, 2830.
[13] A. H. Lu, E. L. Salabas, F. Schuth, *Angew. Chem.* **2007**, *119*, 1242; *Angew. Chem. Int. Ed.* **2007**, *46*, 1222.
[14] Y. W. Jun, J. W. Seo, A. Cheon, *Acc. Chem. Res.* **2008**, *41*, 179.
[15] N. A. Frey, S. Peng, K. Cheng, S. H. Sun, *Chem. Soc. Rev.* **2009**, *38*, 2532.
[16] Y. H. Deng, D. W. Qi, C. H. Deng, X. M. Zhang, D. Y. Zhao, *J. Am. Chem. Soc.* **2008**, *130*, 28.
[17] H. H. P. Yiu, H. J. Niu, E. Biermans, G. van Tendeloo, M. J. Rosseinsky, *Adv. Funct. Mater.* **2010**, *20*, 1599.
[18] E. Q. Song, J. Hu, C. Y. Wen, Z. Q. Tian, X. Yu, Z. L. Zhang, Y. B. Shi, D. W. Pang, *ACS Nano* **2011**, *5*, 761.

[19] Y. Chen, H. R. Chen, S. J. Zhang, F. Chen, L. X. Zhang, J. M. Zhang, M. Zhu, H. X. Wu, L. M. Guo, J. W. Feng, J. L. Shi, *Adv. Funct. Mater.* **2011**, *21*, 270.
[20] B. Luo, S. Xu, A. Luo, W. R. Wang, S. L. Wang, J. Guo, Y. Lin, D. Y. Zhao, C. C. Wang, *ACS Nano* **2011**, *5*, 1428.
[21] J. Liu, S. Z. Qiao, Q. H. Hu, G. Q. Lu, *Small* **2011**, *7*, 425.
[22] J. Liu, B. Wang, S. B. Hartono, T. T. Liu, P, Kantharidis A. P. J. Middelberg, G. Q. Lu, L. Z. He, S. Z. Qiao, *Biomaterials* **2012**, *33*, 970.
[23] Y. W. Jun, J. H. Lee, J. Cheon, *Angew. Chem.* **2008**, *120*, 5200; *Angew. Chem. Int. Ed.* **2008**, *47*, 5122.
[24] H. P. Cong, J. J. He, Y. Lu, S. H. Yu, *Small* **2010**, *6*, 169.
[25] H. Tan, J. M. Xue, B. Shuter, X. Li, J. Wang, *Adv. Funct. Mater.* **2010**, *20*, 722.
[26] H. X. Wu, S. J. Zhang, J. M. Zhang, G. Liu, J. L. Shi, L. X. Zhang, X. Z. Cui, M. L. Ruan, Q. J. He, W. B. Bu, *Adv. Funct. Mater.* **2011**, *21*, 1850.
[27] F. Tan, Y. Zhang, W. Mi, J. Wang, J. Wei, Y. Cai, X. Qian, *J. Proteome Res.* **2008**, *7*, 1078.
[28] L. Zhang, S. Z. Qiao, Y. G. Jin, H. G. Yang, S. Budihartono, F. Stahr, Z. F. Yan, X. L. Wang, Z. P. Hao, G. Q. Lu, *Adv. Funct. Mater.* **2008**, *18*, 3203.
[29] Y. H. Deng, C. H. Deng, D. W. Qi, C. Liu, J. Liu, X. M. Zhang, D. Y. Zhao, *Adv. Mater.* **2009**, *21*, 1377.
[30] H. M. Chen, C. H. Deng, X. M. Zhang, *Angew. Chem.* **2010**, *122*, 617; *Angew. Chem. Int. Ed.* **2010**, *49*, 607.
[31] S. S. Liu, H. M. Chen, X. H. Lu, C. H. Deng, X. M. Zhang, P. Y. Yang, *Angew. Chem.* **2010**, *122*, 7719; *Angew. Chem. Int. Ed.* **2010**, *49*, 7557.
[32] W. F. Ma, Y. Zhang, L. L. Li, L. J. You, P. Zhang, Y. T. Zhang, J. M. Li, M. Yu, J. Guo, H. J. Lu, C. C. Wang, *ACS Nano* **2012**, *6*, 3179.
[33] J. Ptacek, G. Devgan, G. Michaud, H. Zhu, X. W. Zhu, J. Fasolo, H. Guo, G. Jona, A. Breitkreutz, R. Sopko, R. R. McCartney, M. C. Schmidt, N. Rachidi, S. J. Lee, A. S. Mah, L. Meng, M. J. R. Stark, D. F. Stern, C. De Virgilio, M. Tyers, B. Andrews, M. Gerstein, B. Schweitzer, P. F. Predki, M. Snyder, *Nature* **2005**, *438*, 679.
[34] J. V. Olsen, B. Blagoev, F. Gnad, B. Macek, C. Kumar, P. Mortensen, M. Mann, *Cell* **2006**, *127*, 635.
[35] E. L. Huttlin, M. P. Jedrychowski, J. E. Elias, T. Goswami, R. Rad, S. A. Beausoleil, J. Villen, W. Haas, M. E. Sowa, S. P. Gygi, *Cell* **2010**, *143*, 1174.
[36] X. Q. Xu, C. H. Deng, M. X. Gao, W. J. Yu, P. Y. Yang, X. M. Zhang, *Adv. Mater.* **2006**, *18*, 3289.
[37] C. S. Pan, M. L. Ye, Y. G. Liu, S. Feng, X. G. Jiang, G. H. Han, J. J. Zhu, H. F. Zou, *J. Proteome Res.* **2006**, *5*, 3114.
[38] Y. C. Li, Y. S. Lin, P. J. Tsai, C. T. Chen, W. Y. Chen, Y. C. Chen, *Anal. Chem.* **2007**, *79*, 7519.
[39] H. J. Zhou, S. Y. Xu, M. L. Ye, S. Feng, C. S. Pan, X. G. Jiang, X. Li, G. H. Han, Y. Fu, H. F. Zou, *J. Proteome Res.* **2006**, *5*, 2431.
[40] S. Feng, M. L. Ye, H. J. Zhou, X. G. Jiang, X. N. Jiang, H. F. Zou, B. L. Gong, *Mol. Cell. Proteomics* **2007**, *6*, 1656.
[41] H. J. Zhou, M. L. Ye, J. Dong, G. H. Han, X. N. Jiang, R. N. Wu, H. F. Zou, *J. Proteome Res.* **2008**, *7*, 3957.
[42] P. Y. Wang, L. Zhao, R. Wu, H. Zhong, H. F. Zou, J. Yang, Q. H. Yang, *J. Phys. Chem. C* **2009**, *113*, 1359.
[43] Z. Y. Yu, G. H. Han, S. T. Sun, X. N. Jiang, R. Chen, F. J. Wang, R. A. Wu, M. L. Ye, H. F. Zou, *Anal. Chim. Acta* **2009**, *636*, 34.
[44] J. Y. Wei, Y. J. Zhang, J. L. Wang, F. Tan, J. F. Liu, Y. Cai, X. H. Qian, *Rapid Commun. Mass Spectrom.* **2008**, *22*, 1069.
[45] D. W. Qi, Y. Mao, J. Lu, C. H. Deng, X. M. Zhang, *J. Chromatogr. A* **2010**, *1217*, 2606.
[46] J. Lu, Y. Li, C. H. Deng, *Nanoscale* **2011**, *3*, 1225.
[47] F. Bai, X. L. Yang, W. Q. Huang, *Macromolecules* **2004**, *37*, 9746.
[48] P. L. Stanghellini, E. Boccaleri, E. Diana, G. Alberti, R. Vivani, *Inorg. Chem.* **2004**, *43*, 5698.
[49] G. Nonglaton, I. O. Benitez, I. Guisle, M. Pipelier, J. Leger, D. Dubreuil, C. Tellier, D. R. Talham, B. Bujoli, *J. Am. Chem. Soc.* **2004**, *126*, 1497.
[50] X. D. Yao, A. Freas, J. Ramirez, P. A. Demirev, C. Fenselau, *Anal. Chem.* **2001**, *73*, 2836.
[51] W. F. Ma, S. Xu, J. M. Li, J. Guo, Y. Lin, C. C. Wang, *J. Polym. Sci., Part A: Polym. Chem.* **2011**, *49*, 2725.